Enhanced collective focusing of intense neutralized ion beam pulses in the presence of weak solenoidal magnetic fields[a)]

Mikhail A. Dorf,[1,b)] Ronald C. Davidson,[2] Igor D. Kaganovich,[2] and Edward A. Startsev[2]
[1]*Lawrence Livermore National Laboratory, Livermore, California 94550, USA*
[2]*Plasma Physics Laboratory, Princeton, New Jersey 08543, USA*

(Received 2 December 2011; accepted 10 April 2012; published online 31 May 2012)

The design of ion drivers for warm dense matter and high energy density physics applications and heavy ion fusion involves transverse focusing and longitudinal compression of intense ion beams to a small spot size on the target. To facilitate the process, the compression occurs in a long drift section filled with a dense background plasma, which neutralizes the intense beam self-fields. Typically, the ion bunch charge is better neutralized than its current, and as a result a net self-pinching (magnetic) force is produced. The self-pinching effect is of particular practical importance, and is used in various ion driver designs in order to control the transverse beam envelope. In the present work we demonstrate that this radial self-focusing force can be significantly enhanced if a weak ($B \sim 100\,G$) solenoidal magnetic field is applied inside the neutralized drift section, thus allowing for substantially improved transport. It is shown that in contrast to magnetic self-pinching, the enhanced collective self-focusing has a radial electric field component and occurs as a result of the overcompensation of the beam charge by plasma electrons, whereas the beam current becomes well-neutralized. As the beam leaves the neutralizing drift section, additional transverse focusing can be applied. For instance, in the neutralized drift compression experiments (NDCX) a strong (several Tesla) final focus solenoid is used for this purpose. In the present analysis we propose that the tight final focus in the NDCX experiments may possibly be achieved by using a much weaker (few hundred Gauss) magnetic lens, provided the ion beam carries an equal amount of co-moving neutralizing electrons from the preceding drift section into the lens. In this case the enhanced focusing is provided by the collective electron dynamics strongly affected by a weak applied magnetic field. © *2012 American Institute of Physics*. [http://dx.doi.org/10.1063/1.4722999]

I. INTRODUCTION

The high efficiency of energy delivery and deposition makes intense ion beam pulses particularly attractive for high energy density physics applications, and recent advances in ion accelerators and focusing systems have made possible the production of high energy density conditions and warm dense matter (WDM) phenomena under controlled laboratory conditions.[1–5] For instance, WDM density-temperature regimes similar to the interiors of giant planets and low-mass stars are accessible in compact beam-driven experiments.[1,2] Furthermore, in addition to fundamental physics applications, the use of intense heavy ion beams for compression and heating of a target fuel is a promising approach to inertial confinement fusion energy applications.[1–5]

An intense high energy ion beam is produced and delivered to the target by an *ion driver*, as shown in the schematic in Fig. 1. Leaving the ion source, an ion beam pulse is matched into the accelerator region, where the directed kinetic energy of the beam ions is significantly increased. The transverse confinement of the ion beam in the accelerator section against strong space-charge forces is typically provided by a periodic focusing lattice consisting of quadrupole or solenoidal focusing magnetic or electrostatic lenses. In order to increase the intensity of the long ion beam pulse, temporal and spatial compression occurs in the subsequent compression section. For this purpose, leaving the acceleration section, the radially convergent ion beam pulse acquires a head-to-tail velocity tilt and propagates through a long drift section filled with a dense background plasma, which charge neutralizes the ion charge bunch, and hence facilitates compression of the charge bunch against strong space-charge forces. Finally, additional focusing is provided in the final focus section, and then the compressed ion bunch deposits its energy into the target.

Although a full-scale heavy ion fusion test facility with high-gain target physics is presently in a design stage, a compact heavy ion driver for warm dense matter experiments (neutralized drift compression experiment (NDCX-I)) was built at the Lawrence Berkeley National Laboratory.[6,7] In this ion-beam-driven experiment a $\sim 300\,keV$ Potassium (K^+) ion beam pulse undergoes simultaneous ($\sim$50X longitudinal, and $\sim$10X) radial compression, and deposits its energy within $\sim 2.5\,ns$ in $\sim 1.5\,mm$ focal spot, carrying a current of $\sim 1.5\,A$.[6] While a target temperature of only 0.2 eV – 0.5 eV is expected to be achieved on the NDCX-I facility, its planned upgrade (NDCX-II) will operate at higher beam energies (~ 2 MeV Li^+ ions), and will allow for target heating up to 1–2 eV by delivering a $\sim 1\,ns$ compressed bunch carrying a current of $\sim 30\,A$.[8]

[a)]Paper PI3 4, Bull. Am. Phys. Soc. **56**, 229 (2011).
[b)]Invited speaker.

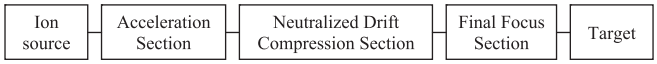

FIG. 1. Block diagram of an ion driver for ion-beam-driven warm dense matter and high energy density physics applications, and inertial confinement fusion.

The control over the transverse beam envelope during its neutralized drift compression and subsequent final focusing is of particular importance for the driver performance. In the present work we discuss the possibility of improving the beam pulse transverse transport properties using weak solenoidal magnetic fields, and analyze the results for the parameters characteristic of the NDCX-I and its planned upgrade (NDCX-II).

A. Enhanced self-focusing of an ion beam pulse propagating through a background plasma along a solenoidal magnetic field

Typically, as the long ion beam pulse propagates through the neutralized drift section, its charge is better neutralized than its current, and as a result a net self-pinching (magnetic) force is produced. The effects of self-pinching become most pronounced when the beam radius is small compared to the collisionless plasma electron skin depth, $r_b < c/\omega_{pe}$.[9] In this case the beam current is almost unneutralized, and the self-magnetic field is a maximum. Here, ω_{pe} is the electron plasma frequency, and c is the speed of light *in vacuo*. The self-pinching effect is of particular practical importance, and is used in various ion driver designs in order to control the transverse beam envelope.[10–13] In particular, in order to reduce the size and cost of the final focusing system as well as to relax the constraint on momentum spread in the accelerator system, it has been proposed to remove the strong transverse focusing upstream of the compression section, and then let the beam propagate through a neutralized compression section as a magnetic self-pinch.[10]

The idea of utilizing self-pinch transport in a driver design can become even more attractive in view of recent findings[14,15] demonstrating that for an ion beam with $r_b < c/\omega_{pe}$ the self-focusing force can be significantly enhanced if a moderately weak solenoidal field satisfying

$$\omega_{ce} \gg \beta_b \omega_{pe} \tag{1}$$

is applied along the beam propagation direction. Here, ω_{ce} is the electron cyclotron frequency and $\beta_b = V_b/c$ is the normalized ion beam velocity. The threshold value of the magnetic field in the inequality (1) can be expressed as $B_c = \beta_b (n_p[cm^{-3}]/10^{11})^{1/2} kG$, corresponding to a relatively weak magnetic field of order 50 G for ion beams with $\beta_b \sim 0.05$ propagating through a background plasma with density $n_p \sim 10^{11}\,\mathrm{cm}^{-3}$. It is important to note that in contrast to magnetic self-pinching, the enhanced collective self-focusing has a dominating radial self-electric field component and occurs as a result of the overcompensation of the beam charge by the plasma electrons, whereas the beam current becomes well-neutralized.[14,15]

Finally, we note that the fringe fields of the strong final focus magnetic solenoid can penetrate deeply into the drift section providing conditions for the enhanced self-focusing to occur. This can significantly influence the neutralized ion beam transport, making studies of the enhanced self-focusing effects in the presence of weak solenoidal magnetic fields of particular practical importance. In particular, for the design parameters of the NDCX-II experiment the effect of the plasma-induced self-focusing provided by the magnetic fringe fields penetrating inside the drift section can become comparable to the focusing effect of the strong final focus solenoid.[14,15]

In the present work (Sec. II), we (a) provide a detailed discussion of this enhanced self-focusing phenomenon; (b) determine the self-consistent evolution of the transverse beam pulse envelope for the case of a parabolic radial beam density profile; (c) assess the influence of the background plasma electron thermal effects on the beam self-focusing; and finally, (d) discuss the feasibility of describing the enhanced self-focusing within the electrostatic approximation, which is often used in numerical codes for ion beam transport simulations.

B. Collective focusing lens for the beam final focus

Typically, in order to provide final transverse beam focusing, a strong (several Tesla) magnetic solenoid placed downstream of the drift section is involved in the design of an ion driver (e.g., NDCX-I and NDCX-II). Due to the strong space-charge self-fields of an intense ion beam pulse, a neutralizing plasma is required inside the magnetic solenoid. Note that apart from the challenge of using a several Tesla magnetic solenoid, filling it with a background plasma provides additional technical challenges.[16] However, the technical realization of the final beam focus can be significantly simplified if the collective focusing scheme (hereafter referred to as a collective focusing lens) is used.[17,18] In particular, a much weaker magnetic field (several hundred Gauss) would be required to achieve the same final focal length.

In the collective focusing scheme originally proposed and experimentally tested by Robertson,[19,20] an ion beam pulse enters a magnetic lens carrying an equal amount of comoving neutralizing electrons. Note that in contrast to conventional neutralized magnetic focusing, no preformed plasma is required, and in fact should not be present inside the lens.[21] Due to the collective electron dynamics inside the lens, a strong ambipolar radial electric field develops that provides a focusing force acting on the beam ions, which is substantially larger than the magnetic $V \times B$ focusing force. As a result, the focusing strength of the lens is significantly enhanced, and for a given magnetic field, the focal length of the collective focusing lens is a factor of $m_i/m_e^{1/2}$ smaller than the focal length of the conventional magnetic lens. Here, m_e is the electron mass, and m_i is the mass of the beam ions.

The feasibility of using a collective focusing lens for final beam focusing has been recently demonstrated in numerical simulations showing that a tight final focus in the NDCX-I experiments can be achieved by using a several hundred Gauss magnetic lens (instead of presently used 8 T

solenoid).[17,18] Note that the NDCX-I configuration conveniently allows the ion beam pulse to extract neutralizing electron background from the plasma that fills the magnetic-field-free drift section.

In the present work (Sec. III), we discuss details and limitations of the collective focusing scheme, and present the results of advanced numerical simulations demonstrating the feasibility of the tight final beam focusing for the parameters of the NDCX-II experiment.

The present paper is organized as follows. The enhanced self-focusing of an ion beam pulse propagating through a background plasma along a solenoidal magnetic field is discussed in Sec. II. Section III presents the analysis of the collective focusing lens, in which an ion beam pulse enters a magnetic lens carrying an equal amount of co-moving neutralizing electrons. The focusing effects described in Sec. II and Sec. III are compared in Sec. IV. Finally, the conclusions of the present work are summarized in Sec. V.

II. ENHANCED SELF-FOCUSING OF AN ION BEAM PROPAGAITING THROUGH A MAGNETIZED PLASMA

In this section we consider an ion beam pulse propagating through a pre-formed dense neutralizing plasma along a solenoidal magnetic field. The significant difference from the "unmagnetized case" with no applied magnetic field is that a small radial displacement, δr, of a background plasma electron is now accompanied by a strong azimuthal rotation of the electron around the beam axis. Indeed, due to the conservation of canonical angular momentum for the case of an azimuthally symmetric ion beam, variations of magnetic flux through the electron orbit set up a large kinetic component of the canonical angular momentum, i.e., the electrons start to rotate about the beam axis (axis of symmetry of the beam-plasma system) with a high azimuthal velocity $V_{e\varphi}$ (Fig. 2). Because the $V_{e\varphi} \times B_z$ force should be mostly balanced by a radial self-electric field, the electron rotation results in a polarization of the plasma and produces a much larger self-electric field than in the limit with no applied field.[14,15,22,23]

It has been also found that the properties of the background plasma response are significantly different depending on whether the value of the solenoidal magnetic field is below or above the threshold value specified by $\omega_{ce}^{cr} = 2\beta_b \omega_{pe}$. The paramagnetic plasma response and the defocusing effect of a radial self-electric field, generated due to a local polarization of the magnetized plasma background, have been demonstrated for the case where $\omega_{ce} < 2\beta_b \omega_{pe}$.[22] In contrast, for the case where $\omega_{ce} > 2\beta_b \omega_{pe}$, the plasma response is diamagnetic, and the radial self-electric field is focusing.[14,15]

A plausible heuristic description of qualitatively different regimes of ion beam interaction with the background plasma can be given, based on the analysis of the balance between the electric and magnetic forces acting on a rotating background plasma electron (Fig. 2). Figure 2(a) shows the case of under-neutralized beam space-charge corresponding to $\omega_{ce} < 2\beta_b \omega_{pe}$. In this regime the net positive charge of the ion beam attracts a plasma electron, i.e., $\delta r < 0$. Due to conservation of canonical angular momentum, a decrease in the magnetic flux through the electron orbit provides electron angular rotation in the negative azimuthal direction, $V_{e\varphi} < 0$. As a result, the radial component of the magnetic force acting on the electron is positive, $f_M = -eB_0 V_{e\varphi}/c > 0$, and is balanced by the positive (defocusing) radial component of the electric field, $E_r > 0$. Note that the positive azimuthal component of the electron current, $j_{e\varphi} = -en_e V_{e\varphi} > 0$, produces a positive (paramagnetic) perturbation of the longitudinal magnetic field, $\delta B_z > 0$. In contrast, for the case where the beam space charge is over-neutralized [Fig. 2(b)] a plasma electron moves radially outward as the ion beam approaches, i.e., $\delta r > 0$, and an increase in the magnetic flux is associated with the positive azimuthal component of the electron velocity, $V_{e\varphi} > 0$. This leads to a diamagnetic effect, $\delta B_z < 0$, and also a focusing self-electric field, $E_r < 0$, is generated to provide force balance on the plasma electrons. The enhanced self-focusing force provided by this strong radial electric is calculated in the following section (Sec. II A).

It is interesting to note that the qualitatively different local plasma responses are separated by the critical value of magnetic field, specified by $\omega_{ce} = \omega_{ce}^{cr}$, which corresponds to the resonant excitation of large-amplitude wave-field perturbations (whistler waves).[15,24] The excited wave-field perturbations propagate oblique to the beam with characteristic longitudinal wave number $k_z \sim l_b^{-1}$, where l_b is the characteristic beam length. Therefore, their contribution to the total Lorentz force can have opposite signs for the beam head and the beam tail, leading to the distortion of the beam pulse shape. However, for a long beam pulse with $l_b \gg \max\{r_b, V_b/\omega_{pe}\}$, it has been demonstrated for the case where $\omega_{ce} \gg$

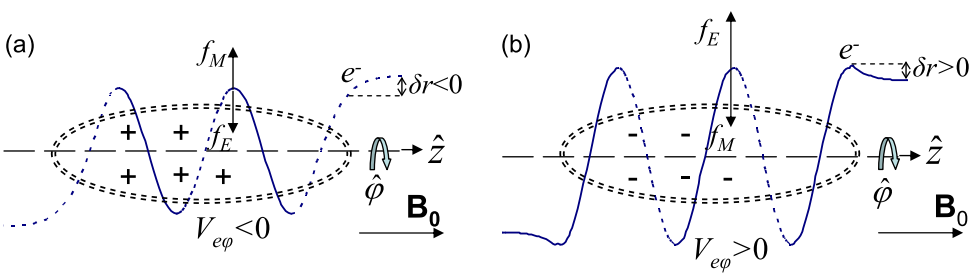

FIG. 2. Two different regimes of ion beam interaction with a background plasma. (a) Corresponds to $\omega_{ce} < 2\beta_b \omega_{pe}$; the beam charge is under-neutralized, the radial self-electric field is defocusing, $E_r > 0$, and the plasma response is paramagnetic, $\delta B_z > 0$. (b) Corresponds to $\omega_{ce} > 2\beta_b \omega_{pe}$; the beam charge is overneutralized, the radial self-electric field is focusing, $E_r < 0$, and the plasma response is diamagnetic, $\delta B_z < 0$. The blue curves illustrate the trajectory of a background plasma electron; the double-dashed lines illustrate the outline of the ion charge bunch; and $f_E = -eE_r$ and $f_M = -(e/c)V_{e\varphi}B_0$.

$2\beta_b\omega_{pe}$ and the beam radius is not too small, $r_b \gg V_b(1+\omega_{ce}^2/\omega_{pe}^2)^{1/2}/\omega_{ce}$, the radial focusing force provided by wave-field perturbations, which extend far outside the beam, become negligible compared to the focusing force provided by the local plasma polarization.[15] Finally, note that no whistler wave-field perturbations are excited for the case where $\omega_{ce} < 2\beta_b\omega_{pe}$.[15,22,23]

A. Radial focusing force calculation

In order to analyze the self-focusing effect quantitatively, we now derive a general expression for the radial component of the Lorentz force,[14]

$$F_r = Z_b e(E_r - \beta_b B_\varphi), \tag{2}$$

acting on the ion beam pulse propagating through a background plasma along a uniform magnetic field $\mathbf{B_0} = B_0\mathbf{z}$. Here, B_φ and E_r are the azimuthal component of the magnetic field, and the radial component of the electric field, respectively; and Z_b is the charge state of the beam ions. For simplicity, we assume immobile plasma ions, ballistic (infinitely heavy) beam ions, cold plasma electrons and investigate the axisymmetric steady-state solution where all quantities depends on t and z solely through the combination $\xi = z - V_b t$. Assuming that the beam density is small compared to the electron density ($n_b \ll n_e$), we solve for the linear plasma response, in which the plasma electron dynamics is governed to leading order in the cold-plasma approximation by

$$m_e V_b \frac{\partial \mathbf{V_e}}{\partial \xi} = \frac{e}{c}[\mathbf{V_e} \times \mathbf{B_0}] + e\mathbf{E}. \tag{3}$$

Here, $\mathbf{V_e}$ is the electron flow velocity and we have made use of $\partial/\partial t = -V_b\partial/\partial\xi$ for the steady-state electron response. Applying the curl operator to the both sides of Eq. (3) and making use of Faraday law, we readily obtain

$$m_e V_b \frac{\partial}{\partial \xi}\left(\nabla \times \mathbf{V_e} - \frac{e}{m_e c}\mathbf{B}\right) = \frac{e}{c}\nabla \times [\mathbf{V_e} \times \mathbf{B_0}]. \tag{4}$$

Combining the φ-component of Eq. (4) with the r-component of Eq. (3) yields[14]

$$F_r = Z_b e E_r - \frac{Z_b e}{c} V_b B_\varphi = Z_b m_e V_b \frac{\partial V_{ez}}{\partial r}. \tag{5}$$

For a long ion beam pulse with $r_b \ll l_b$ and $\omega_{pe} l_b/V_b \gg 1$ it was first demonstrated by making use of the slice approximation,[14] and then confirmed in a more detailed analysis accounting for the effects of coupling between the longitudinal and transverse dynamics[15] that for the case where the beam radius is greater than the effective electron gyroradius, r_{ge}, i.e.,

$$r_b \gg r_{ge} \equiv \frac{V_b}{\omega_{ce}}\left(1+\omega_{ce}^2/\omega_{pe}^2\right)^{1/2}, \tag{6}$$

the beam current becomes fully-neutralized, i.e., $n_e V_{ez} = Z_b n_b V_b$. For this case it readily follows from Eq. (5) that the radial focusing force is given in the linear approximation, i.e., $n_b \ll n_e$, by

$$F_r = Z_b^2 m_e V_b^2 \frac{1}{n_e}\frac{\partial n_b}{\partial r}. \tag{7}$$

It is straightforward to show that the ratio of the collective self-focusing force in the presence of an applied magnetic field [Eq. (7)] to the self-pinching force, F_0, occurring for $B_0 = 0$ can be estimated for the case where the magnetic self-pinching force is maximum, i.e. $r_b \ll c/\omega_{pe}$, as[14,15]

$$F_r/F_0 \sim (c/r_b\omega_{pe})^2 \gg 1. \tag{8}$$

Note that for the case where $\omega_{ce} \gg \beta_b\omega_{pe}$ the condition in Eq. (6) can be satisfied even in the limit $r_b \ll c/\omega_{pe}$. Figure 3 shows the results of illustrative electromagnetic particle-in-cell (PIC) simulation demonstrating a significant increase in the self-focusing force in the presence of a weak magnetic field. Note that excellent agreement with the theoretical predictions in Eq. (7) is obtained.

Finally, we emphasize again that for the case where the conditions for enhanced focusing to occur are satisfied [Eqs. (1) and (6)] the beam current becomes well-neutralized, leading to $B_\varphi \approx 0$, and therefore the dominant contribution to the self-focusing force in Eq. (7) comes from the radial self-electric field. For instance, for the parameters of the numerical simulation shown in Fig. (3), the contribution of the electric component to the total Lorentz force constitutes more than 99%.

B. Self-consistent analysis of the transverse beam focusing

It is of particular practical importance to investigate the self-consistent evolution of the ion beam radial density profile under the influence of the radial self-focusing force described by Eq. (7). As an illustrative example, we present here a self-consistent analytic solution describing the transverse beam focusing for the case of a cold ion beam with a parabolic density profile.

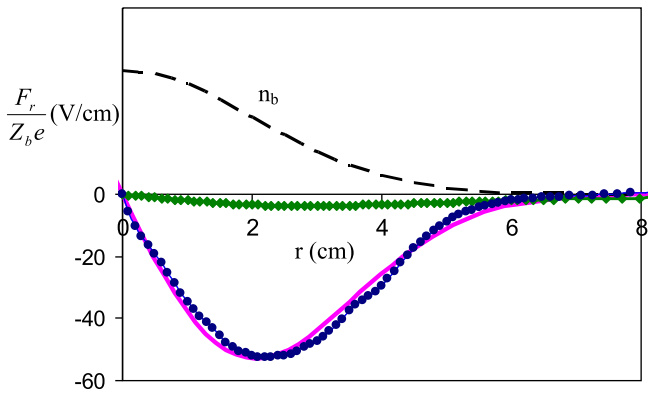

FIG. 3. Radial dependence of the normalized focusing force at the beam center.[14] The results of the numerical simulations correspond to $B_0 = 300$ G and $\omega_{ce}/\beta_b\omega_{pe} = 18.7$ (blue circles), and $\omega_{ce} = 0$ (green diamonds). The analytical results in Eq. (7) are shown by the solid pink curve. The beam parameters correspond to $Z_b = 1$, $r_b = 0.55\, c/\omega_{pe}$, $l_b = 1.875\, c/\omega_{pe}$, $\beta_b = 0.05$, and the plasma density is taken to be $n_p = 10^{10}\,\mathrm{cm}^{-3}$. The dashed black curve corresponds to the radial beam density profile, $n_b = 0.14 n_p \exp[-r^2/r_b^2 - (z - V_b t)^2/l_b^2]$. Results are obtained using the cylindrical (r, z) version of the LSP code.[25]

Assuming azimuthal symmetry, the transverse dynamics of a long ion beam pulse is governed by

$$\frac{\partial n}{\partial t}+\frac{1}{r}\frac{\partial}{\partial r}(rnV_r)=0, \tag{9}$$

$$\frac{\partial V_r}{\partial t}+V_r\frac{\partial V_r}{\partial r}=\alpha\frac{\partial n}{\partial r}, \tag{10}$$

where $n(r,t)$ is the ion beam density, $V_r(r,t)$ is the radial component of the ion fluid velocity, $\alpha=Z_b^2m_eV_b^2/(m_bn_e)$, m_b is the mass of the beam ions, n_e is the background electron density, and we have neglected the terms involving the longitudinal derivatives, $\partial/\partial z\approx 0$. For the case of a parabolic density profile, it is straightforward to show that

$$n(r,t)=\begin{cases} n_{b0}(t)\dfrac{R_{b0}^2}{R_b^2(t)}\left(1-\dfrac{r^2}{R_b^2(t)}\right), & r<R_b(t) \\ 0, r\geq R_b(t), \end{cases} \tag{11}$$

and

$$V_r(r,t)=-U(t)\frac{r}{R_b(t)}, \tag{12}$$

where R_{b0} and n_0 describe the initial beam radius and the on-axis number density, respectively. Equations (11) and (12) constitute solutions to Eqs. (9) and (10), provided the time-dependent functions R_b(t) and U(t) satisfy

$$\frac{dR_b}{dt}=-U(t) \tag{13}$$

and

$$\frac{dU}{dt}=2\alpha n_{b0}\frac{R_{b0}^2}{R_b^3(t)}. \tag{14}$$

Assuming there is no initial convergence, i.e., $U(t=0)=0$, it follows that the evolution of the beam radius, R_b(t), is given by

$$R_b(t)=R_{b0}\sqrt{1-2\frac{\alpha n_{b0}}{R_{b0}^2}t^2}. \tag{15}$$

From Eq. (15) it follows for the case where the conditions for the enhanced focusing to occur [see Sec. II A] are satisfied that an ion beam pulse with a parabolic density profile propagating through a dense background plasma along a magnetic field will come to a radial focus at

$$L_f=\frac{R_{b0}}{\sqrt{2}Z_b}\sqrt{\frac{m_bn_e}{m_en_{b0}}}. \tag{16}$$

C. Thermal effects of the background plasma electrons

In previous sections the ion beam self-focusing has been analyzed, assuming cold neutralizing background. Here, we investigate the influence of the plasma electron thermal effects on the beam self-focusing. It is important to note that apart from the heating produced inside the plasma source, significant additional electron heating may be provided by the ion beam pulse as a result of collective (beam-plasma) streaming instabilities.[26–28]

Assuming, for simplicity, a scalar form of the electron pressure, $p_e=n_eT_e$, the radial component of the electron force balance equation [Eq. (3)] is given in the linear approximation, $n_b\ll n_e$, by

$$m_eV_b\frac{\partial V_e}{\partial\xi}=\frac{e}{c}V_{e\varphi}B_0+eE_r+\frac{1}{n_e}\frac{\partial p_e}{\partial r}. \tag{17}$$

The effects of electron pressure become important for the case where $\partial p_e/\partial r\sim n_eeE_r$. Making use of Eq. (7) to estimate the radial electric field and assuming that $\partial p_e/\partial r\sim T_e\partial n_e/\partial r$, it follows that the electron thermal effects become pronounced for the case where the electron temperature reaches the characteristic value, T_{ec}, given by

$$T_{ec}\frac{\partial n_e}{\partial r}\sim Z_bm_eV_b^2\frac{\partial n_b}{\partial r}. \tag{18}$$

Estimating the variations in the electron density, $\delta n_e=n_e-n_p$, for the case of a long ion beam pulse from $r^{-1}\partial(rE_r)/\partial r\approx 4\pi e(Z_bn_b-\delta n_e)$, where n_p is the unperturbed uniform background plasma density and Eq. (7) is used to determine the radial electric field, it follows that

$$\frac{\partial n_e}{\partial r}\sim Z_b\frac{\partial n_b}{\partial r}\left(1+\frac{V_b^2}{\omega_{pe}^2r_b^2}\right). \tag{19}$$

Note that the ratio $V_b^2/\omega_{pe}^2r_b^2$ determines the degree of the ion beam charge overcompensation by the neutralizing plasma background.[23] Finally, making use of Eqs. (18) and (19), it readily follows that

$$T_{ec}\sim m_eV_b^2(1+V_b^2/\omega_{pe}^2r_b^2)^{-1}. \tag{20}$$

As the electron temperature increases, one should expect to observe a decrease in the enhanced self-focusing force. Indeed, the strong radial electric field that constitutes most of the focusing is generated to balance the magnetic $V_{e\varphi}\times B_0$ force acting on the azimuthally rotating electrons (Sec. II A). However, in the presence of the electron thermal pressure part of the magnetic force is balanced by the pressure force, therefore requiring a weaker radial electric field to provide radial electron force balance.

The influence of the electron thermal effects on the radial focusing electric field have been studied with the LSP PIC code,[25] and the results of the illustrative simulation are shown in Fig. 4. It is readily seen that an increase in the electron temperature leads to a decrease in the focusing electric field, and the characteristic value of the electron temperature for which thermal effects become pronounced is in good agreement with the estimate in Eq. (20).

D. Electrostatic model of the enhanced self-focusing

The results discussed in the previous sections [e.g., Eqs. (6) and (7)] have been obtained in Refs. 14 and 15 by taking

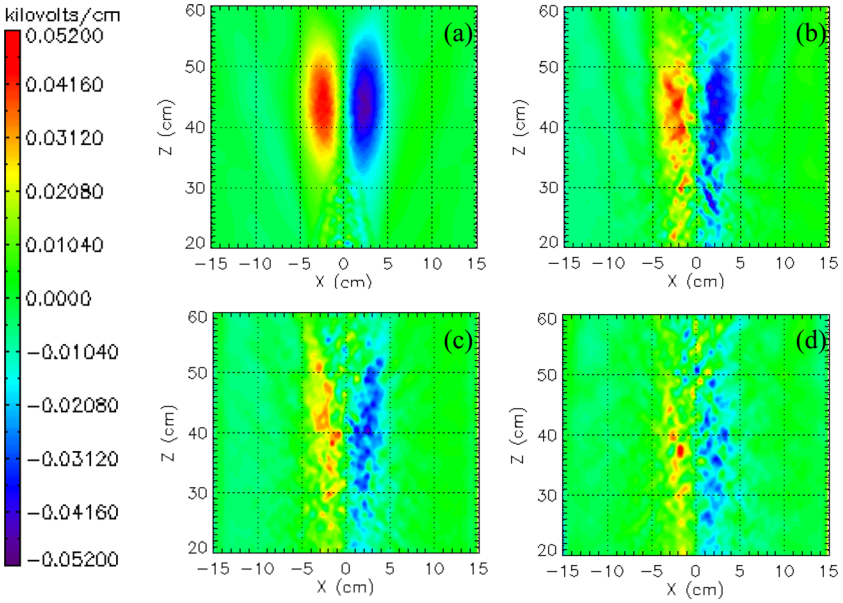

FIG. 4. Influence of plasma electron thermal effects on the transverse beam self-focusing. Shown are plots of the transverse self-electric field corresponding to (a) $T_e = 0$ eV, (b) $T_e = 300$ eV, (c) $T_e = 600$ eV, and (d) $T_e = 1000$ eV. The beam parameters correspond to $Z_b = 1$, $r_b = 0.55\, c/\omega_{pe}$, $l_b = 1.875\, c/\omega_{pe}$, $\beta_b = 0.05$, the plasma density is $n_p = 10^{10}\,\mathrm{cm}^{-3}$, and the applied magnetic field corresponds to $B_0 = 300$ G. The black curve corresponds to the radial beam density profile, $n_b = 0.13 n_p \exp[-r^2/r_b^2 - (z - V_b t)^2/l_b^2]$. The characteristic value of the electron temperature given by Eq. (20) corresponds to $T_{ec} = 1255$ eV. Results are obtained using the slab (x, z) version of the LSP code.[25]

into account electromagnetic effects in describing the dynamics of background plasma electrons. It is however interesting to note that the self-focusing force specified by Eq. (7) can be obtained within an electrostatic model provided the condition in Eq. (6) is satisfied. The electrostatic approximation is often used in numerical codes for simulations of a heavy ion driver (e.g., the electrostatic version of the WARP code[29]), and therefore this result can be of particular practical importance.

As in previous sections, we consider here immobile plasma ions, cold background plasma electrons, and assume a linear electron response, which is valid provided $n_b \ll n_e$. The axisymmetric steady-state solution where all quantities depends solely on the combination $\xi = z - V_b t$ is described in the electrostatic approximation by the cold-fluid equations for electrons

$$-V_b \frac{\partial}{\partial \xi}\delta n_e + n_p \frac{1}{r}\frac{\partial}{\partial r} r V_{er} + n_p \frac{\partial}{\partial \xi} V_{ez} = 0, \tag{21}$$

$$-m_e V_b \frac{\partial V_{e\varphi}}{\partial \xi} = \frac{e}{c} V_{er} B_0, \tag{22}$$

$$-m_e \mathrm{V}_b \frac{\partial V_{er}}{\partial \xi} = e\frac{\partial \varphi}{\partial r} - \frac{e}{c} V_{e\varphi} B_0, \tag{23}$$

$$-m_e V_b \frac{\partial V_{ez}}{\partial \xi} = e\frac{\partial \varphi}{\partial \xi}, \tag{24}$$

and Poisson's equation for the electrostatic field, $\mathbf{E} = -\nabla\varphi$

$$\frac{\partial^2}{\partial \xi^2}\varphi + \frac{1}{r}\frac{\partial}{\partial r}\left(r\frac{\partial}{\partial r}\varphi\right) = -4\pi e(Z_b n_b - \delta n_e). \tag{25}$$

Here, $\delta n_e = n_e - n_p$, where n_p is the unperturbed plasma density outside from the beam, and we have made use of $\partial/\partial t = -V_b \partial/\partial \xi$ and $\partial/\partial z = \partial/\partial \xi$ for the steady-state electron response. Finally, note that in the linear approximation, the magnetic $V_e \times B$ force corresponding to the magnetic field perturbations is of second order in n_b/n_e, and therefore does not appear in Eqs. (22) and (23).

From Eqs. (22) and (23) it follows that

$$\frac{1}{\omega_{ce}} m_e V_b^2 \frac{\partial^2}{\partial \xi^2} V_{e\varphi} = e\frac{\partial}{\partial r}\varphi - \frac{e}{c} V_{e\varphi} B_0. \tag{26}$$

Assuming that the ion beam pulse is sufficiently long with $l_b \gg V_b/\omega_{ce}$, we readily obtain

$$V_{e\varphi} = \frac{c}{B_0}\frac{\partial}{\partial r}\varphi \tag{27}$$

and

$$V_{er} = -\frac{cV_b}{\omega_{ce} B_0}\frac{\partial}{\partial \xi}\frac{\partial}{\partial r}\varphi. \tag{28}$$

Combining Eqs. (28), (24), and (21) yields

$$-V_b \frac{\partial}{\partial \xi}\delta n_e - \frac{n_p}{r}\frac{\partial}{\partial r}\left(r\frac{cV_b}{\omega_{ce} B_0}\frac{\partial}{\partial \xi}\frac{\partial}{\partial r}\varphi\right) - \frac{n_p e}{m_e V_b}\frac{\partial}{\partial \xi}\varphi = 0. \tag{29}$$

Making use of Poisson's equation (25) and assuming $\partial^2/\partial \xi^2 \sim 1/l_b^2 \ll \omega_{pe}^2/V_b^2$ we obtain

$$\left(1 + \frac{\omega_{pe}^2}{\omega_{ce}^2}\right)\frac{1}{r}\frac{\partial}{\partial r}\left(r\frac{\partial}{\partial r}\varphi\right) + \frac{\omega_{pe}^2}{V_b^2}\varphi = -4\pi Z_b e n_b. \tag{30}$$

It now follows from Eq. (30) for the case where $r \gg r_{ge} \equiv (V_b/\omega_{ce})(1 + \omega_{ce}^2/\omega_{pe}^2)^{1/2}$ that

$$e\varphi = -Z_b m_e V_b^2 \frac{n_b}{n_p}, \tag{31}$$

and we readily obtain the electrostatic radial focusing force, $F_{sf}^{el} = -Z_b e \partial\varphi/\partial r$, consistent with the results of the general analysis [see Eq. (7)].

It should be noted, however, that the analysis presented in this section only demonstrates that in the limit $r \gg r_{ge}$ the electrostatic model predicts the same electric field as that obtained in the generalized analysis for the case where $\omega_{ce} \gg 2\beta_b\omega_{pe}$ and $r \gg r_{ge}$.[14,15] Additional analysis has to be performed in order to determine the regime of validity of the electrostatic approximation. It should be noted that for the case where $\omega_{ce} < 2\beta_b\omega_{pe}$ the return electron current is driven primarily by the inductive electric field;[22,23] and for the case where $\omega_{ce} \approx 2\beta_b\omega_{pe}$ large-amplitude electromagnetic wave fields can be excited.[15,24] These effects are not described by the electrostatic model. We emphasize here that electrostatic numerical codes are often used for simulations of an ion driver, and it is therefore of particular practical importance to identify the conditions where the electrostatic modeling can adequately describe the ion beam dynamics inside the neutralized drift section. This will be a subject of future studies.

III. COLLECTIVE FOCUSING LENS FOR THE BEAM FINAL FOCUS

In the previous section it was shown that even a weak solenoidal magnetic field of order 100 G can have a significant influence on the dynamics of an intense ion beam pulse propagating through a neutralizing background plasma. In particular, analytical calculations and numerical simulations demonstrated enhanced ion beam self-focusing induced by the collective dynamics of the plasma electrons. However, it should also be pointed out that the collective effects of a neutralizing electron background in a weak solenoidal magnetic field were also utilized in a magnetic focusing scheme proposed by S. Robertson a few decades ago.[19] In this section we review this focusing scheme, discuss extension of the original theoretical model,[17] and finally, asses the possibility of its implementation for final focusing of intense ion beams in the NDCX-II.

A. Collective focusing lens

In the collective focusing scheme proposed and experimentally tested by Robertson,[19] an ion beam pulse enters a magnetic lens carrying an equal amount of co-moving neutralizing electrons. The neutralizing electrons entering the lens experience much stronger magnetic focusing than the beam ions and tend to build up a negative charge around the lens axis. As a result, an electrostatic ambipolar electric field develops that significantly increases the total focusing force acting on the beam ions.

The collective focusing force acting on the beam ions can be calculated as follows.[17,19] We consider a neutralized ion beam pulse moving from a region of a zero magnetic field into a solenoidal magnetic lens. As the charge particles traverse the field fall-off region, where the magnetic field has a non-zero radial component they acquire angular rotation around the lens axis. From conservation of canonical radial momentum it then follows that inside the lens the species azimuthal velocity is given by $V_\alpha^\phi = r_\alpha\Omega_\alpha/2$. Here, the subscripts $\alpha = e, i$ denote electrons or ions, respectively, r_α is the radial coordinate of a particle of species α, and $\Omega_\alpha = q_\alpha B_0/m_\alpha c$, where B_0 is the magnetic field inside the lens, and q_α and m_α are the species charge and mass, respectively. It is then straightforward to show that the evolution of a particle's radial coordinate inside the lens is governed by

$$\frac{d^2}{dt^2}r_\alpha + \frac{1}{4}r_\alpha\Omega_\alpha^2 - \frac{q_\alpha}{m_\alpha}E_r = 0. \tag{32}$$

In the original derivation for the case of a quasi-neutral ion beam focusing,[19] identical radial motion of the electrons and the ions was assumed, i.e., $r_e(z,t) = r_i(z,t)$, which yields in the limit $m_e \ll m_i$

$$\frac{d^2}{dt^2}r_\alpha + \frac{1}{4}Z_b r_\alpha\Omega_e\Omega_i = 0, \tag{33}$$

and the strong ambipolar electric field that provides the enhanced collective focusing is given by

$$E_r = -m_e\Omega_e^2\frac{r}{4e}. \tag{34}$$

Here, $Z_b = q_i/e$ denotes the ion charge state. It is important to note that the electric field in Eq. (34) is generated to balance the magnetic $V_e^\theta \times B_0$ force and the centrifugal force acting on neutralizing electrons inside the lens. It therefore follows that in order for collective focusing to occur, no pre-formed neutralizing plasma or secondary electrons should be present inside the lens. Otherwise, the rotating electrons co-moving with the ion beam will be rapidly replaced by the "non-rotating" background plasma (or secondary) electrons inside the lens, and the enhanced collective focusing will be suppressed.[21]

From Eq. (34) it follows that the focal length of a collective lens in the *thin* lens limit, i.e., for the case where the radial displacement of the beam particles within the lens is small, is given by

$$L_f^{coll} \cong 4Z_b^{-1}V_b^2/(\Omega_e\Omega_i L_s), \tag{35}$$

where L_s is the lens length. Note that the focal length of a "conventional" magnetic lens is given in the thin-lens approximation for a single-species ion beam by

$$L_f^m \cong 4V_b^2/(\Omega_i^2 L_s). \tag{36}$$

Equation (36) follows from Eq. (32), assuming that $E_r \cong 0$, provided the beam space-charge is weak or well-neutralized by a preformed background plasma. Comparing Eqs. (35) and (36) it follows that for a given focal length, the magnetic field required for the collective focusing is smaller by a factor of $\sqrt{m_i/m_e}$.

In the derivation of Eqs. (33) and (34) it has been assumed that (a) the collective focusing is quasi-neutral, and (b) the magnetic field perturbations, which are mainly created by the azimuthal electron current, are small. It is straightforward to show that the quasi-neutrality is maintained provided the electron beam is sufficiently dense that[17,19]

$$\omega_{pe}^2 \gg \frac{1}{2}\Omega_e^2, \tag{37}$$

and the magnetic perturbations are small provided the beam radius is small compared to the collisionless electron skin depth[17,19]

$$\frac{1}{2}r_b \ll \frac{c}{\omega_{pe}}. \tag{38}$$

Here, $\omega_{pe}^2 = 4\pi e^2 n_e/m_e$ is the electron plasma frequency, $n_e = Z_b n_b$ is the electron density, and n_b is the ion beam density.

However, it is also of considerable practical interest to investigate the effects of enhanced collective focusing in extended parameter regimes. In particular, it may be of great interest to utilize the collective focusing concept in the laser generation of a high-energy ion beam, where the energetic ions are produced and accelerated by the interaction of an intense laser beam pulse with a thin foil.[30,31] Along with the ions, a free-moving electron background is also produced, and therefore it is appealing to utilize the collective focusing concept for collimation of the generated ion beam pulse.[17] However, in these applications the ion beam radius is typically larger than the collisionless electron skin depth, and therefore the condition in Eq. (38) is violated. Also, propagation of a neutralized (by co-moving electrons) ion beam along a strong solenoidal magnetic field with $\Omega_e > \omega_{pe}$ can occur both in a heavy ion driver[6] and in the laser production of collimated ion beams[31] when a conventional (several Tesla) magnetic lens is used for ion beam focusing.

A detailed analysis of collective focusing for the cases where $\Omega_e > \omega_{pe}$ or $r_b > c/\omega_{pe}$ was performed in Ref. 17, by making use of reduced analytical models and advanced numerical simulations. In particular, it was demonstrated for the case where $\Omega_e > \omega_{pe}$ that *nonneutral* compression corresponding to an excess of negative charge near the solenoidal axis can occur. For the case of strong nonneutral compression, with $n_e \gg Z_b n_i$ near the beam axis, it has been shown that the electron beam radius decreases approximately as $R_e \propto 1/\omega_{ce}$, where ω_{ce} is the local value of the electron cyclotron frequency. The radial electric field inside the electron beam, $r < R_e$, is found to be linear with $E_r = -m_e\omega_{ce}^2(z)r/4e$, and the reduced self-consistent analytical model describing the nonlinearities in the radial electric for $r > R_e$ has been derived.[17] In addition, for the case where $r_b > c/\omega_{pe}$ the perturbation in the solenoidal magnetic field produced by the azimuthal component of the electron beam current has been calculated self-consistently, and a significant suppression of the applied magnetic has been demonstrated. However, it is found that even for large values of $r_b\omega_{pe}/c$, the outer edge of the ion beam pulse can still experience efficient collective focusing.[17]

In conclusion, we comment on the "thermal" limits of the collective focusing arising from the quasi-adiabatic heating of the co-moving electrons.[18,20] As the effective electron temperature increases during compression, the electron thermal pressure becomes more pronounced, and balances part of the magnetic electron focusing force. As a result, the radial electric field required to provide radial electron force balance decreases, vanishing to zero at the electron stagnation point where[18]

$$T_{es} \sim m_e\omega_{ce}^2 R_{es}^2/4. \tag{39}$$

Here, T_{es} and R_{es} are the effective electron temperature and the beam radius at the stagnation point. Assuming that the effective electron transverse emittance is approximately constant during the compression, i.e. $R_0^2 T_{e0} \sim R_{es}^2 T_{es}$, where T_{e0} and R_0 denote the initial values of the effective electron temperature and the beam radius, the radius of the ion beam focal spot, R_{bf}, can be estimated as

$$R_{bf} \sim R_{es} \sim \left(\frac{4R_0^2 T_{e0}}{m_e\omega_{ce}^2}\right)^{1/4}. \tag{40}$$

For example, for $R_0 = 1$ cm, $T_{e0} = 5$ eV, and $B_0 = 1$ kG the estimate in Eq. (40) gives $R_{bf} \sim 1$ mm. Finally, we note that the value of the electron temperature predicted in Eq. (39) along with quasi-adiabaticity of the electron compression, i.e., $R_0^2 T_{e0} \sim R_{es}^2 T_{es}$, was observed (approximately) in the numerical simulations in Ref. 18.

B. Collective focusing lens for NDCX-II final focus

In this section we propose a conceptual design of the NDCX-II final focus section that demonstrates the feasibility of tight, collective final beam focusing. In the schematic shown in Fig. (5), an ion beam pulse passes through a final focus solenoid as it leaves the neutralized drift section (see Fig. 5). The beam is allowed to extract the electrons when leaving the plasma layer should the forces on them induce such motion, and is expected to be well-neutralized.[17,18,32–35] In the idealized simulations presented here, the upstream effects of the radial and longitudinal beam convergence are not taken into account, and the following initial beam parameters are considered: the injected beam density is $n_{b0} = 5 \times 10^{10}\,\mathrm{cm}^{-3}$; the directed energy of the beam ions is $E_b = 2$ MeV; the ion beam radius is $r_{b0} = 0.5$ cm; the duration of the ion beam pulse is $\tau \approx 10$ ns; and the transverse and longitudinal beam temperatures are assumed to be $T_b = 0.2$ eV. To model the short downstream part of the neutralizing drift section, a carbon plasma layer is placed between $z = 0$ cm and $z = 12$ cm. The plasma density is assumed to be uniform with $n_p = 4 \times 10^{11}\,\mathrm{cm}^{-3}$, and the electron and ion temperatures are taken to be $T_{e0} = T_{i0} = 3$ eV. Figure 6 presents the initial illustrative results of the numerical particle-in-cell simulations performed using the LSP code,[25] and demonstrating the feasibility of a tight collective focus for the case where the magnetic field inside the final focus solenoid is $B_0 = 900$ G. The ion beam comes to a tight focus at $z_f \sim$

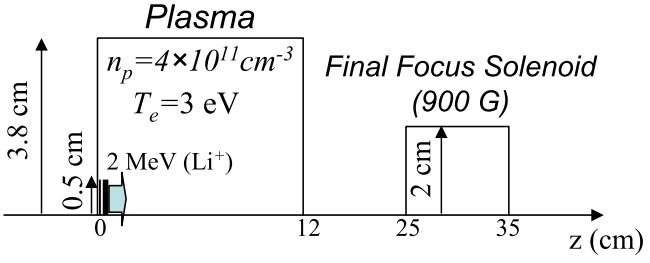

FIG. 5. Schematic of conceptual design of the NDCX-II final focus section used for the idealized numerical LSP simulations.

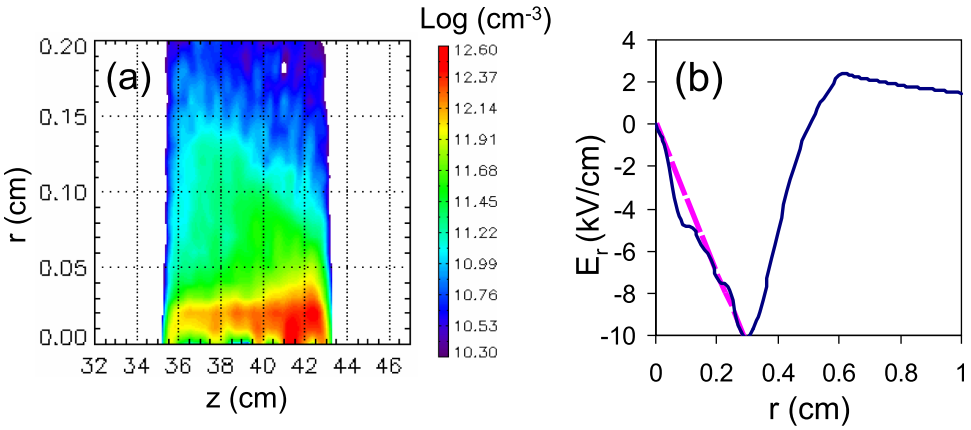

FIG. 6. Results of the numerical simulations performed with the cylindrical (r, z) electromagnetic version of the LSP code for the idealized model of the NDCX-II final beam focus. Shown in the figure are: (a) Plot of the ion beam density at the focal plane corresponding to $t = 58$ ns and (b) radial dependence of the radial electric field inside the lens corresponding to $z = 30$ cm and $t = 45$ ns (solid blue line). The analytical results in Eq. (34) are shown by the pink dashed line in Frame (b).

42 cm, with ~80 times increase in the beam number density, $n_f \sim 4 \times 10^{12}\,\mathrm{cm}^{-3}$ [Fig. 6(a)]. The radial electric field inside the lens is shown in Fig. 6(b), and agrees well with the analytical predictions in Eq. (34).

In conclusion, the collective final focusing scheme can be naturally utilized in the NDCX experiments, where a neutralizing co-moving electron background can be extracted from the neutralizing drift section, and then only a moderately weak magnetic lens (several hundred Gauss) is required for a tight beam focus. We emphasize again that the use of the collective scheme for the final beam focusing removes many of the challenges in operating a strong magnetic solenoid (several Tesla) and filling it with a background plasma.

IV. PLASMA INDUCED SELF-FOCUSING VERSUS COLLECTIVE FOCUSING LENS

It is of considerable interest to compare the focusing effect of a collective focusing lens (Sec. III) to the enhanced self-focusing of an ion beam propagating through a background neutralizing plasma along a solenoidal magnetic field (Sec. II). For both cases, the enhanced focusing is provided by a strong radial self-electric field, which is produced to balance the magnetic $V \times B$ force acting on the rotating neutralizing electrons. Note, however, that for the case of a collective focusing lens, a rotation of the co-moving electrons is acquired due to variations of the applied solenoidal magnetic field, from zero outside the lens to the maximum value inside the lens. In contrast, for the case of plasma-induced self-focusing, the background plasma electrons are initially immersed in an applied magnetic field, and variations of the magnetic flux that determines the electron rotation are associated with a small radial displacement of the electron orbits in the presence of the ion beam self-fields. For this reason, plasma-induced enhanced self-focusing can occur even for the case of a uniform applied magnetic field. In contrast, in order for the enhanced focusing to occur inside a collective focusing lens, the neutralized beam has to traverse the fall-off region of a solenoidal field. Moreover, note that the value of the plasma-induced self-focusing force [Eq. (7)] does not depend on the local value of the applied magnetic field. The value of the applied magnetic field however determines the conditions for the enhanced self-focusing to occur [see Eqs. (1) and (6)]. Finally, the important feature of the collective focusing lens is that it provides a linear (in radius) focusing force for the case of quasi-neutral compression. In contrast, the plasma-induced self-focusing force is proportional to the beam density gradient, $F_{sf} \propto \partial n_b/\partial r$, and therefore its radial profile can be strongly non-linear. However, note that this feature of the self-focusing force can be of particular importance for ion beam self-pinch transport applications, where the defocusing effects provided by the ion beam thermal pressure have to be compensated.

The ratio of the focusing force acting on the beam ions inside a collective focusing lens, F_{coll}, to the plasma-induced self-focusing force in the presence of an applied magnetic field, F_{sf}, can be estimated as

$$\frac{F_{coll}}{F_{sf}} \sim \frac{1}{4}\frac{r_b^2\Omega_e^2}{V_b^2}. \tag{41}$$

In obtaining the estimate in Eq. (41), it has been assumed that $\partial/\partial r \sim 1/r_b$ and $Z_b n_b \sim n_p$ in the expression for the plasma-induced self-focusing force [Eq. (7)]. It is interesting to note that in the limit where the beam radius is the order of $r_b \sim V_b/\Omega_e$, which correspond to the threshold value in the condition in Eq. (6) for $\Omega_e \ll \omega_{pe}$, the effects become of the same order, i.e., $F_{coll} \sim F_{sf}$.

Finally, we comment on the significant suppression of the total focusing effect that has been observed in the experiments in Ref. 21 when a neutralizing plasma was produced inside a collective focusing lens. Although enhanced plasma-induced self-focusing could still occur inside the magnetic lens due to the presence of the background plasma, its influence on the ion beam dynamics would be much less than the original effects of the collective focusing lens. Indeed, a simple calculation shows that for the parameters of the experiments in Ref. 21, where a 360 keV proton beam with $r_b \sim 2$ cm passes through a collective lens with $B_0 \sim 1$kG, the effective electron gyroradius is small, $r_{ge} = V_b/\Omega_e \sim 0.05$ cm, and the ratio in Eq. (41) is much greater than unity, $F_{coll}/F_{sf} \sim 428$. However, note that for the design parameters of a heavy-ion fusion driver, where the beam energy can correspond to $\beta_b \sim 0.6$,[36] both focusing effects generated in an applied magnetic field of ~1 kG become comparable for $r_b \sim 1$ cm.

V. CONLCLUSIONS

In the present paper we considered two schemes for intense ion beam focusing, which utilize the collective

dynamics of neutralizing electrons. In the first approach, the ion beam propagates through a neutralizing background plasma along a uniform magnetic field (enhanced plasma-induced self-focusing). In the second approach, the ion beam passes through a finite size plasma, extracts neutralizing electrons from the plasma, and then enters a magnetic lens (collective focusing lens). Note that for this focusing scheme to work, the beam has to extract the neutralizing electrons from a region of a zero magnetic field, and no background plasma or secondary electrons should be present inside the lens. In both cases, a strong radial electric field is produced due to the collective electron dynamics. This self-electric field provides the enhanced transverse focusing of the beam ions. Detailed analytical and advanced numerical studies using particle-in-cell simulations were performed for both approaches and their application for the beam focusing in the Neutralized Drift Compression Experiments (NDCX-I and NDCX-II) were discussed.

In particular, a detailed discussion of the enhanced plasma-induced self-focusing including the approximate analytical derivation of the focusing force and its verification in the advanced numerical simulations were presented. In addition, an analytical solution describing the self-consistent evolution of the transverse beam envelope during self-focusing was obtained for the case of a parabolic radial beam density profile. Also, the thermal effects of the background plasma electrons were investigated. It was shown that the radial electric field, which provides most of the self-focusing force, significantly decreases when the electron temperature becomes comparable to $T_e \sim m_e V_b^2 (1 + V_b^2/\omega_{pe}^2 r_b^2)^{-1}$. Finally, it was shown that the effect of enhanced self-focusing can be recovered within the electrostatic approximation.

We also reviewed the concept of the collective focusing lens, including an extension of the original analysis to the regime of non-neutral compression corresponding to $\omega_{ce} > \omega_{pe}$, and the regime where pronounced perturbations of the applied magnetic field can occur (corresponding to $r_b > \omega_{pe}/c$). In addition, we proposed a conceptual design of the NDCX-II final focus section, for which the feasibility of tight, collective final beam focusing was demonstrated in the advanced numerical simulations described in this paper.

ACKNOWLEDGMENTS

This work was performed under the auspices of the U.S. Department of Energy by the University of California, Lawrence Livermore National Laboratories under Contract No. DE-AC52-07NA27344, and by the Princeton Plasma Physics Laboratory under Contract No. DE-AC02-76CH-O3073.

[1]R. C. Davidson, *Frontiers in High Energy Density Physics – The X-Games of Contemporary Science* (National Academies Press, 2002).
[2]B. G. Logan, F. M. Bieniosek, C. M. Celata, J. Coleman, W. Greenway, E. Henestroza, J. W. Kwan, E. P. Lee, M. Leitner, P. K. Roy, P. A. Seidl, J.-L. Vay, W. L. Waldron, S. S. Yu, J. J. Barnard, R. H. Cohen, A. Friedman, D. P. Grote, M. Kireeff Covo, A. W. Molvik, S. M. Lund, W. R. Meier, W. Sharp, R. C. Davidson, P. C. Efthimion, E. P. Gilson, L. Grisham, I. D. Kaganovich, H. Qin, A. B. Sefkow, E. A. Startsev, D. Welch, and C. Olson, Nucl. Instrum. Methods Phys. Res. A **577**, 1 (2007).
[3]B. Yu. Sharkov, Nucl. Instrum. Methods Phys. Res. A **577**, 14 (2007).
[4]K. Horioka, T. Kawamura, M. Nakajima, K. Kondo, M. Ogawa, Y. Oguri, J. Hasegawa, S. Kawata, T. Kikuchi, T. Sasaki, M. Murakami, and K. Takayama, Nucl. Instrum. Methods Phys. Res. A **606**, 1 (2009).
[5]D. H. H. Hoffmann, V. E. Fortov, M. Kuster, V. Mintsev, B. Y. Sharkov, N. A. Tahir, S. Udrea, D. Varentsov, and K. Weyrich, Astrophys. Space Sci. **322**, 167 (2009).
[6]P. A. Seidl, A. Anders, F. M. Bieniosek, J. J. Barnard, J. Calanog, A. X. Chen, R. H. Cohen, J. E. Coleman, M. Dorf, E. P. Gilson, D. P. Grote, J. Y. Jung, M. Leitner, S. M. Lidia, B. G. Logan, P. Ni, P. K. Roy, K. VandenBogert, W. L. Waldron, and D. R. Welch, Nucl. Instrum. Methods Phys. Res. A **606**, 75 (2009).
[7]P. K. Roy, S. S. Yu, E. Henestroza, A. Anders, F. M. Bieniosek, J. Coleman, S. Eylon, W. G. Greenway, M. Leitner, B. G. Logan, W. L. Waldron, D. R. Welch, C. Thoma, A. B. Sefkow, E. P. Gilson, P. C Efthimion, and R. C. Davidson, Phys. Rev. Lett. **95**, 234801 (2005).
[8]A. Friedman, J. J. Barnard, R. H. Cohen, D. P. Grote, S. M. Lund, W. M. sharp, A. Faltens, E. Henestroza, J.-Y. Jung, J. W. Kwan, E. P. Lee, M. A. Leitner, B. G. Logan, J.-L. Vay, W. L Waldron, R. C. Davidson, M. Dorf, E. P. Gilson, and I. D. Kaganovich, Phys. Plasmas **17**, 056704 (2010).
[9]I. D. Kaganovich, G. Shvets, E. Startsev, and R. C. Davidson, Phys. Plasmas **8**, 4180 (2001).
[10]K. Hahn and E. Lee, Fusion Eng. Des. **32–33**, 417 (1996).
[11]D. R. Welch and C. L. Olson, Fusion Eng. Des. **32–33**, 477 (1996).
[12]C. L. Olson, Nucl. Instrum. Methods Phys. Res. A **464**, 118 (2001).
[13]P. F. Ottinger, Phys. Plasmas **7**, 346 (2000).
[14]M. Dorf, I. Kaganovich, E. Startsev, and R. Davidson, Phys. Rev. Lett. **103**, 075003 (2009).
[15]M. Dorf, I. Kaganovich, E. Startsev, and R. C. Davidson, Phys. Plasmas **17**, 023103 (2010).
[16]P. K. Roy, P. A. Seidl, A. Anders, F. M. Bieniosek, J. E. Coleman, E. P. Gilson, W. Greenway, D. P. Grote, J. Y. Jung, M. Leitner, S. M. Lidia, B. G. Logan, A. B. Sefkow, W. L. Waldron, and D. R. Welch, Nucl. Instrum. Methods Phys. Res. A **606**, 22 (2009).
[17]M. Dorf, I. Kaganovich, E. Startsev, and R. C. Davidson, Phys. Plasmas **18**, 033106 (2011).
[18]M. Dorf, I. D. Kaganovich, E. A. Startsev, and R. C. Davidson, in *Proceedings of the 2010 International Accelerator Conference*, Kyoto, Japan, 2010, p. 4635.
[19]S. Robertson, Phys. Rev. Lett. **48**, 149 (1982).
[20]S. Robertson, J. Appl. Phys. **59**, 1765 (1986).
[21]R. Kraft, B. Kusse, and J. Moschella, Phys. Fluids **30**, 245 (1987).
[22]I. D. Kaganovich, E. A. Startsev, A. B. Sefkow, and R. C. Davidson, Phys. Rev. Lett. **99**, 235002 (2007).
[23]I. D. Kaganovich, R. C. Davidson, M. A. Dorf, E. A. Startsev, A. B. Sefkow, A. F. Friedman, and E. P. Lee, Phys. Plasmas **17**, 056703 (2010).
[24]A. Volokitin, C. Krafft, and G. Matthieussent, Phys. Plasmas **2**, 4297 (1995).
[25]LSP is a software product developed by ATK Mission Research, Albuquerque, NM 87110.
[26]E. A. Startsev, R. C. Davidson, and M. Dorf, Phys. Plasmas **15**, 062107 (2008).
[27]R. C. Davidson, M. A. Dorf, I. D. Kaganovich, H. Qin, A. B. Sefkow, E. A. Startsev, D. R. Welch, D. V. Rose, and S. M. Lund, Nuclear Nucl. Instrum. Methods Phys. Res. A **606**, 11 (2009).
[28]R. Lee and R. N. Sudan, Phys. Fluids **14**, 1213 (1971).
[29]A. Friedman, D. P. Grote, and I. Haber, Phys. Fluids B **4**, 2203 (1992).
[30]R. A. Snavely, M. H. Key, S. P. Hatchett, T. E. Cowan, M. Roth, T. W. Phillips, M. A. Stoyer, E. A. Henry, T. C. Sangster, M. S. Singh, S. C. Wilks, A. MacKinnon, A. Offenberger, D. M. Pennington, K. Yasuike, A. B. Langdon, B. F. Lasinski, J. Johnson, M. D. Perry, and E. M. Campbell, Phys. Rev. Lett. **85**, 2945 (2000).
[31]K. Harres, I. Alber, A. Tauschwitz, V. Bagnoud, H. Daido, M. Günther, F. Nürnberg, A. Otten, M. Schollmeier, J. Schütrumpf, M. Tampo, and M. Roth, Phys. Plasmas **17**, 023107 (2010).
[32]S. Humphries, Jr., Appl. Phys. Lett. **32**, 792 (1978).
[33]R. Kraft and B. Kusse, J. Appl. Phys. **61**, 2425 (1987).
[34]D. R. Welch, D. V. Rose, W. M. Sharp, C. L. Olson, and S. S. Yu, Laser Part. Beams **20**, 621 (2002).
[35]W. M. Sharp, D. A. Callahan, M. Tabak, S. S. Yu, P. E. Peterson, D. V. Rose, and D. R. Welch, Nucl. Fusion **44**, 221 (2004).
[36]E. Henestroza, B. G. Logan, and L. J. Perkins, Phys. Plasmas **18**, 032702 (2011).